Supplemental Information Inventory

Figure S1, related to Figure 1. Effect of 5 separate ErbB3 shRNAs on OVCAR8 cell proliferation.

Figure S2, related to Figure 2. EGFR and Her-2 status in ovarian cancer cell lines

Figure S3, related to Figure 3. Effect of NRG1 depletion on ovarian cancer cell lines

Figure S4, related to Figure 5.

Table S1, related to Figure 1. Complete tyrosine kinase shRNA library screening results.

Table S2, related to Figure 2. NRG1/ErbB3 status and shErbB3 sensitivity in ovarian cancer cell lines.

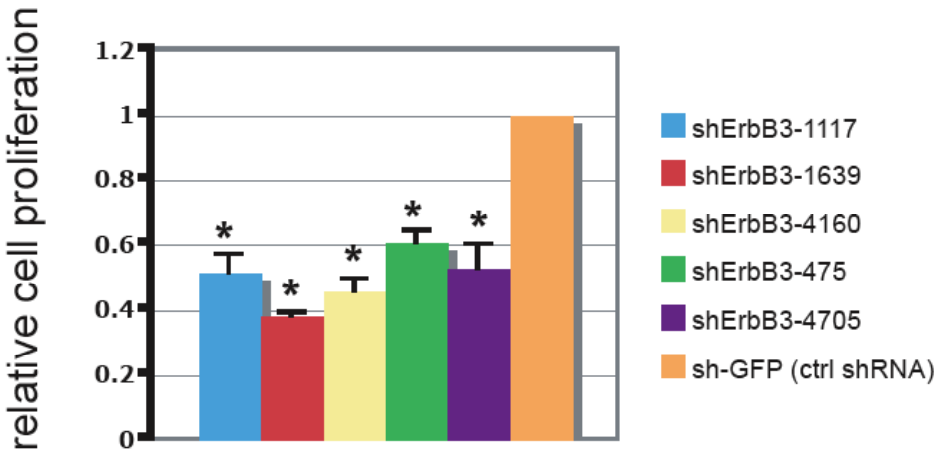

Figure S1. Effect of 5 separate ErbB3 shRNAs on OVCAR8 cell proliferation. (Related to Figure 1.) Depletion of ErbB3 by 5 separate shRNAs resulted in decreased OVCAR8 cell proliferation as assessed by CellTiter-Glo assay. Error bar represents +/- SD.

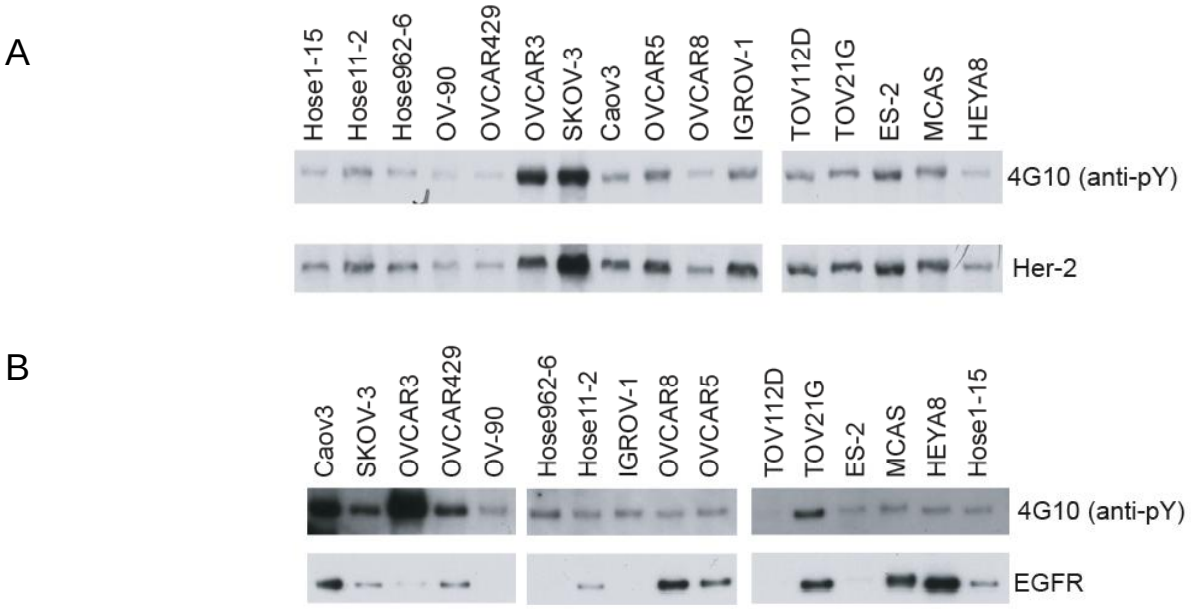

Figure S2. EGFR and Her-2 status in ovarian cancer cell lines. (Related to Figure 2.) Cell lysates from 16 ovarian cancer cell lines were immunoprecipitated with either anti-Her-2 (A) or anti-EGFR (B) antibody followed by blotting with either anti-phosphotyrosine antibody 4G10 (top panels) or anti-Her-2 antibody (A, bottom panel) or anti-EGFR antibody (B, bottom panel).

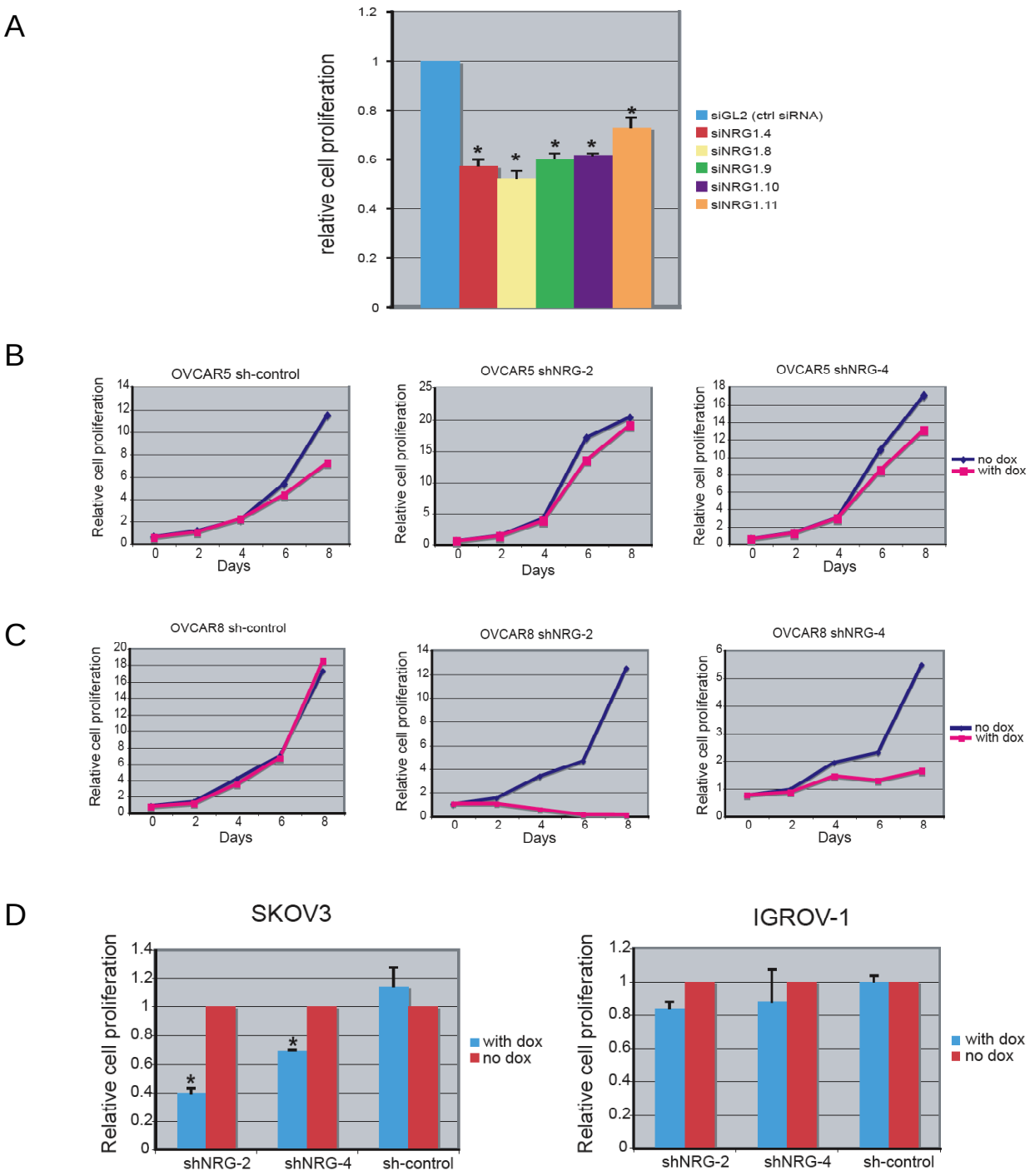

Figure S3. Effect of depletion of NRG1 expression on different ovarian cancer cell lines. (**Related to Figure 3**.) A) Depletion of NRG1 by 5 separate siRNAs resulted in decreased OVCAR8 cell proliferation as assessed by CellTiter-Glo assay. *: values are significantly different from control shRNA or siRNA ($p<0.05$ student's t-test). B) OVCAR5 is insensitive but C) OVCAR8 is sensitive to NRG1 depletion. D) SKOV3 but not IGROV-1 is sensitive to NRG1 depletion. *: $p<0.05$ (student's t-test). Error bars represent +/- SD.

A

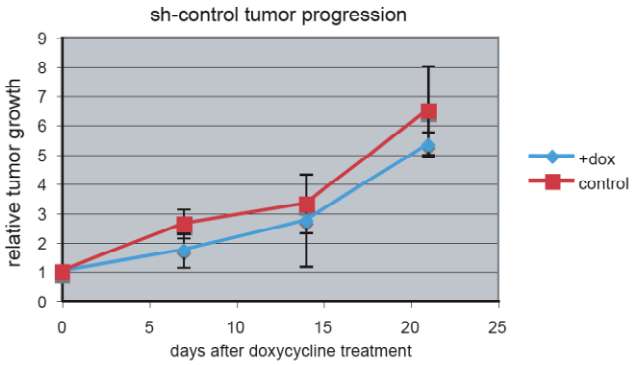

B

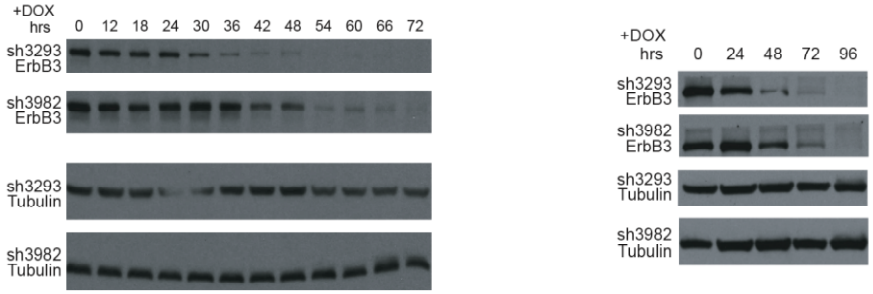

C

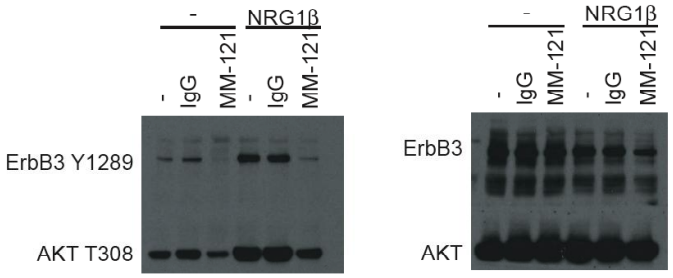

Figure S4. (Related to Figure 5.) A) Growth of intraperitoneally implanted luciferized OVCAR8 cells containing a doxycycline inducible control (scrambled) shRNA in the presence or absence of doxycycline. Tumor growth was monitored by bioluminescence. Error bars represent +/- SEM. B) shErbB3-3293 induces depletion of endogenous ErbB3 earlier than shErbB3-3982 in either 3D spheroid culture or in mouse xenografts. Left panel, ErbB3 protein level from OVCAR8 cells carrying either tet-inducible shErbB3-3293 or shErbB3-3982 in 3D spheroid culture at different time points after addition of doxycycline. Right panel, ErbB3 protein level from OVCAR8 cells carrying either tet-inducible shErbB3-3293 or shErbB3-3982 growing subcutaneously in nude mice at different time points after mice were fed with doxycycline-containing water. In both panels, tubulin served as a protein loading control. C) MM-121 effect on ErbB3 status in OVCAR8 cells. Left panel, MM-121 reduces endogenous as well as NRG1β stimulated ErbB3 phosphorylation. Right panel, MM-121 effect on ErbB3 protein level. Irrelevant human IgG served as a control for MM-121 in these experiments.

Table S2. NRG1/ErbB3 status and sensitivity to shErbB3 in ovarian cancer cell lines. (Related to Figure 2.)

Cell Line	NRG cDNA	ErbB3	Y1289P ErbB3	Sensitivity to shErbB3
OVCAR8	+++	+++	+++	Yes
OVCAR5	-	+++	-	No
OVCAR3	++	+++	++	NT
HEYA8	+	-	-	No
OVCA429	+	+++	+	NT
OVCA420	-	+++	+++	Puro-resistant*
TOV112D	++	+	+	No
IGROV-1	-	++	-	No
CaOV3	+	+++	-	NT
FuOV1	++	+++	-	NT
OV90	+++	++	-	NT
OVCAR432	+	+++	-/+	No
OVCAR433	++	+++	+++	No
ES-2	-	+++	+++	NT
SKOV3	+++	+	+++	Yes
TOV21G	++	++	+++	No

NT = not tested
* Could not be infected with shErbB3 as these cells are intrinsically resistant to puromycin.